Available online at www.sciencedirect.com
ScienceDirect
Polymer 48 (2007) 4087–4096
polymer
www.elsevier.com/locate/polymer

Synthesis and rheological properties of an associative star polymer in aqueous solutions

Sami Hietala [a,*], Pekka Mononen [a], Satu Strandman [a], Paula Järvi [a], Mika Torkkeli [b], Katja Jankova [c], Søren Hvilsted [c], Heikki Tenhu [a]

[a] *Laboratory of Polymer Chemistry, University of Helsinki, P.O. Box 55, FIN-00014 University of Helsinki, Finland*
[b] *Department of Physical Sciences, University of Helsinki, P.O. Box 64, FIN-00014 University of Helsinki, Finland*
[c] *Department of Chemical Engineering, Danish Polymer Center, Technical University of Denmark, Building 423, DK-2800 Kgs. Lyngby, Denmark*

Received 31 January 2007; received in revised form 18 April 2007; accepted 23 April 2007
Available online 5 May 2007

Abstract

Rheological properties of aqueous solutions and hydrogels formed by an amphiphilic star block copolymer, poly(acrylic acid)-*block*-polystyrene (PAA_{54}-*b*-$PS_6)_4$, were investigated as a function of the polymer concentration (C_p), temperature, and added salt concentration. The water-soluble polymer synthesised by atom transfer radical polymerization (ATRP) was found to form hydrogels at room temperature at polymer concentrations, C_p, over 22 g/L due to the interpolymer hydrophobic association of the PS blocks. Increasing C_p leads to stronger elastic networks at room temperature that show a gel-to-solution transition with increasing temperature. Increase of ionic strength decreases the moduli compared with the pure hydrogel but did not affect the gel–sol transition temperature significantly. Small-angle X-ray experiments showed two distinct scattering correlation peaks for samples above the gelling C_p, which indicates the aggregates formed due to hydrophobic association. Upon heating the intensity of the scattering correlation peaks was found to decrease indicating the loss of the network structure due to thermal motion.

Keywords: Star polymer; Water-soluble; Rheology

1. Introduction

Associative polymers are of great industrial importance owing to their adjustable rheological properties, for example in oil recovery, paints, cosmetics formulations and pharmaceutical as well as medical applications such as drug delivery and tissue engineering [1]. Particularly interesting are the stimuli-responsive systems of associating polymers in which free-standing gels transform to free-flowing liquids or vice versa. To obtain such systems water-soluble polymers modified with a small number of hydrophobic groups are often used [2–32]. Enhanced viscosity and reversible gelling behaviour originate from transient intermolecular associations between the hydrophobic groups.

Responsive properties in aqueous solutions are attained by using either neutral (i.e. non-ionizable) water-soluble polymers [4–7,21,30–32] or polyelectrolytes [8–20,22–29]. The self-assembly of block polyelectrolytes gives additional versatility with regards to the responsiveness and polyelectrolytes may create strong elastic gels at lower concentrations than neutral polymers [2]. By changing the polymer concentration [4,6–11,13,14,16–19,26,27], temperature [5,6,15,17,18,21–26], ionic strength [10,27,28], pH [19,29] or by adding analytes [12,23] the solution interactions and the rheological properties may be varied significantly. The characteristics of the polymers may be tuned for example by varying the molar mass of the polymer or the mass ratios of the comonomers, but also by the topology of the polymers, using structures such as

* Corresponding author. Tel.: +358 919150333; fax: +358 919150330.
E-mail address: sami.hietala@helsinki.fi (S. Hietala).

0032-3861/$ - see front matter © 2007 Elsevier Ltd. All rights reserved.
doi:10.1016/j.polymer.2007.04.069

diblocks [2,3,10,14,23,24], triblocks [2,3,6,15–19,25,29] or stars [20,21].

In this work, we have synthesised a relatively monodisperse water-soluble associating starlike polyelectrolyte, four-armed poly(acrylic acid)-*block*-polystyrene, and investigated the stimuli-responsive behaviour of its hydrogels by rheological methods. The starlike topology of the polymer represents a special case of a branched architecture, in which all polymer chains have the same branching point. Compared with linear diblock and triblock polymers the four-armed topology may enable more effective association. Indeed, according to Lin and Cheng [31], four-arm amphiphilic stars based on poly(ethylene oxide) inner blocks and poly(*N*-isopropyl acryl amide) outer blocks are able to form gels that have higher strength than stars with higher number of arms, due to the low intramolecular aggregation in the former case. Another advantage over linear polymer systems is the existence of the central core of the star polymer. Due to the multifunctionality, and often to the hydrophobic nature of the core such polymers have been proposed as carriers for example for fragrance molecules [33], dyes [34] or catalysts [35,36]. The polyelectrolyte core in the present case may also be suitable for encapsulation of ionizable compounds and additionally the polyelectrolyte is sensitive to changes in environmental conditions. Thus in addition to polymer concentration, we have examined the effects of ionic strength and temperature on the rheological properties of the aqueous polymer solutions. Furthermore, small-angle X-ray scattering (SAXS) was used to study the structure of the non-saline polymer solutions at different temperatures.

2. Experimental

2.1. Materials

The synthesis of a tetrafunctional initiator (diTMP–Br) by acylation of di(trimethylolpropane) (diTMP) with 2-bromoisobutyrylbromide is described elsewhere [37]. *tert*-Butyl acrylate and styrene were distilled from CaH_2 prior to use. CuBr, *N*,*N*,*N*′,*N*″,*N*″-pentamethyldiethylenetriamine (PMDETA), trifluoroacetic acid (all from Aldrich) were used without further purification.

2.2. Synthesis of starlike poly(tert-butyl acrylate), $(P(tBA)_4)$

tert-Butyl acrylate (15.34 g, 0.12 mol), CuBr (0.26 g, 1.81 mmol) and diTMP–Br (0.32 g, 0.38 mmol) were placed in a dry Schlenk tube. After dissolving of the initiator (diTMP–Br) the system was degassed by two freeze–thaw cycles under vacuum. PMDETA (0.32 g, 1.85 mmol) was added and three more freeze–thaw cycles were performed. The polymerization was conducted under nitrogen atmosphere at 70 °C for 37 min, after which it was terminated by immersing the tube into liquid nitrogen. The polymer was precipitated in 1:1 water–methanol solution and dried under vacuum at room temperature. The gravimetrically determined conversion was 64%, giving theoretical molar mass M_n(theor) = 26,200 g/mol. The molar mass determined by SEC, M_n(SEC), was 27,000 g/mol, and the corresponding polydispersity was 1.19. The molar mass determined by ^{1}H NMR from the signals of the endgroup, the initiator and the polymer, M_n(NMR), was 27,700 g/mol, and the number of arms was 4. The molar mass determined by static light scattering, M_w(SLS), 65,800 g/mol indicated that some star–star coupling has occurred during the polymerization.

^{1}H NMR (200 MHz, $CDCl_3$) δ ppm: 4.06 (br, 4H) and 3.93 (br, 8H, $-CH_2-$, initiator), 3.25 (br, 4H, $-CH_2O-$, initiator), 2.23 (1H, $-CH-$), 1.80 and 1.75 (2H, $-CH_2-$), 1.75, 1.49 and 1.20 (9H, $-C(CH_3)_3$), 1.11 (9H, $-C(CH_3)$, endgroup), 0.84.

^{13}C NMR (200 MHz, $CDCl_3$) δ ppm: 174.29 (1C, >C=O), 80.46 (1C, $-C(CH_3)_3$), 42.43 and 42.02 (1C, $-CH_2-$), 37.48 and 36.08 (1C, $-CH-$), 28.18 (3C, $-C(CH_3)_3$).

FT-IR (solid, ATR) cm^{-1}: 2997 (w), 2977 (w, $-CH_3$), 2932 (w), 2875 (w, $-CH_3$), 1723 (s, >C=O), 1479 (w, $-CH_3$), 1448 (w), 1392 (m), 1366 (m, $-CH_3$), 1335 (w), 1254 (m, >C=O), 1142 (s, −COOR), 1034 (w), 909 (w), 844 (m), 811 (w), 751 (w).

2.3. Synthesis of starlike poly(tert-butyl acrylate)-block-polystyrene, $(ptBA\text{-}b\text{-}PS)_4$

Starlike poly(*tert*-butyl acrylate) macroinitiator (8.00 g, 0.30 mmol) was dissolved in styrene monomer (50 mL, 45.5 g, 0.45 mol) in a dry Schlenk tube. CuBr (0.18 g, 1.3 mmol) and PMDETA (265 μL, 0.22 g, 1.3 mmol) were added and the solution was degassed by three freeze–thaw cycles under high vacuum. The polymerization was conducted under nitrogen atmosphere at 110 °C for 17 min, after which it was terminated by immersing the tube into liquid nitrogen. The polymer was precipitated in 1:1 water–methanol solution and dried under vacuum at room temperature. The molar mass of the block copolymer M_n(SEC) = 29,000 g/mol and the polydispersity was 1.16. The block copolymer was further purified by fractionation in MeOH at −18 °C, in which the soluble fractions were collected. The molar mass of the combined fractions determined by SEC was 30,300 g/mol and the polydispersity was 1.15. The polystyrene content of the combined fractions was 8.1 mol%, giving M_n(NMR) = 30,100 g/mol.

^{1}H NMR (200 MHz, $CDCl_3$) δ ppm: 7.11 and 6.63 (5H, Ar), 3.94 (br, 8H, $-CH_2-$, initiator), 3.25 (br, 4H, $-CH_2O-$, initiator), 2.24 (1H, $-CH-$, p*t*BA), 1.81 and 1.75 (1H, $-CH-$, PS, and 4H, $-CH_2-$, p*t*BA and PS), 1.49 and 1.25 (9H, $-C(CH_3)_3$), 1.11 (9H, $-C(CH_3)_3$, endgroup), 0.85.

^{13}C NMR (200 MHz, $CDCl_3$) δ ppm: 172.29 (1C, >C=O), 145.32 (1C, Ar), 128.10 (2C, Ar), 125.78 (1C, Ar), 80.46 (1C, $-C(CH_3)_3$), 42.44 and 42.00 (2C, $-CH_2-$, p*t*BA and PS), 40.56 (1C, $-CH-$, PS), 37.50 and 36.07 (1C, $-CH-$, p*t*BA), 28.18 (3C, $-C(CH_3)_3$).

FT-IR (solid, ATR) cm^{-1}: 3002 (w), 2977 (w, $-CH_3$), 2932 (w), 2875 (w, $-CH_3$), 1724 (s, >C=O), 1479 (w, $-CH_3$), 1451 (w), 1392 (m), 1366 (m, $-CH_3$), 1335 (w), 1255 (m, >C=O), 1144 (s, −COOR), 1032 (w), 908 (w), 845 (m), 802 (w), 751 (w), 700 (w, Ar).

2.4. Preparation of starlike poly(acrylic acid)-block-polystyrene, (PAA-b-PS)$_4$

Hydrolysis with trifluoroacetic acid in dichloromethane described by Ma and Wooley [38] was used. Block copolymer was dissolved in dry CH_2Cl_2. Trifluoroacetic acid (5 equiv to the *tert*-butyl ester) was added and the mixture was stirred at room temperature for 24 h. The solution was concentrated by evaporation. (PAA-*b*-PS)$_4$ polymer was dialyzed in a water–acetone mixture (3:1), followed by the dialysis in 0.05 M NaOH solution and in pure water. After the purification, the polymer was lyophilised. According to the ^{1}H NMR spectra both in D_2O and in the mixture of d_6-DMSO and D_2O, the degree of hydrolysis was 97%. Using this degree of hydrolysis, the molar mass of the resulting amphiphilic star copolymer was 23,500 g/mol when calculated from the result by SEC, and 23,100 g/mol when calculated from the result by ^{1}H NMR.

^{1}H NMR (200 MHz, D_2O) δ ppm: 7.27 and 6.91 (5H, Ar), 2.27 (1H, –CH–, PAA), 1.76, 1.62, 1.31, and 1.16, 0.89 (8H, $-CH_2-$, PAA, p*t*BA and PS, as well as –CH–, PS and p*t*BA), 1.45 (9H, $-C(CH_3)_3$, p*t*BA).

FT-IR (solid, ATR) cm^{-1}: 3395 (br, m, –COOH), 3026 (w), 2951(w), 2923 (m), 2853 (w), 2514 (br, w), 1699 (s, >C=O), 1562 (s) and 1550 (s, $-COO^-$), 1491 (w), 1451 (m), 1404 (m, $-COO^-$), 1365 (w), 1279 (br, –COOH), 1248 (s, >C=O), 1170 (s), 1115 (w), 1064 (w), 1050 (w), 1026 (w), 907 (w), 813 (w), 759 (w), 698 (m, Ar).

2.5. Size exclusion chromatography

The SEC analyses were performed with a Waters instrument equipped with a Styragel guard column, 7.8 × 300 mm Styragel capillary column and Waters 2487 UV and Waters 2410 RI detectors. THF was used as an eluent with a flow rate 0.8 mL/min. The calibration was performed either with polystyrene or with poly(methyl methacrylate) standards from PSS Polymer Standards Service GmbH.

2.6. NMR and FT-IR spectroscopy

The conversions of the polymerization of *tert*-butyl acrylate and the compositions of the polymers were determined with a Varian Gemini 2000 NMR spectrometer operating at 200 MHz for ^{1}H NMR and at 50.3 MHz for ^{13}C NMR. The chemical shifts are presented in part per million downfield from the internal TMS standard or with respect to a solvent resonance line. The IR spectra were measured from solid samples with a Perkin Elmer Spectrum One FT-IR spectrometer.

2.7. Rheology

TA AR2000 stress controlled rheometer equipped with 40 mm aluminium 2° cone and a Peltier heated plate were used for the oscillatory and steady shear measurements. Dynamic measurements were made in linear regime at temperatures between 20 and 50 °C. Steady shear measurements were made at 20 °C. In order to probe the temperature dependent rheological properties, heating of the samples was done with a rate of 1 °C/min at oscillation frequency (ω) of 6.283 rad/s or by increasing the temperature in 5 °C steps and measuring the frequency sweep 100–0.1 rad/s at each temperature. The measuring setup was covered with a sealing lid in order to prevent evaporation during the measurement. To prepare samples for rheology and small-angle X-ray scattering, weighed amounts of dry polymer on Teflon-coated glass plates were moistened with deionized water (ELGA PURELAB Ultra) or saline solutions and stored in desiccator overnight. Before measurements a rest period of at least 10 min was employed in order to let the samples stabilise.

2.8. Small angle X-ray scattering

SAXS measurements were made with a setup using sealed anode X-ray tube (Cu-target), multilayer optics with pinhole collimation and a two dimensional position sensitive detector (HISTAR) positioned 50 cm from the sample. The non-saline gel-like samples were sealed in flat 1.5 mm thick cuvettes with thin Mylar films as X-ray windows. The accessible range of scattering vector q was between 0.015 and 0.5 Å^{-1}, where q is calculated from the scattering angle 2θ and wavelength λ (=1.54 Å) as $q = 4\pi/\lambda \sin\theta$. The scattering data were corrected for detector response, spatial resolution and non-sample scattering and azimuthally averaged into 1-D (radial) scattering intensity.

3. Results

3.1. Synthesis and characterisation of the amphiphilic star polymer

The amphiphilic star block copolymer was synthesised by ATRP of *tert*-butyl acrylate, *t*BA, followed by block copolymerisation of styrene and the hydrolysis of poly(*tert*-butyl acrylate) blocks to poly(acrylic acid). The structure and ^{13}C NMR spectrum of the di(trimethylolpropane)-based initiator diTMP–Br used in the polymerization of *t*BA is presented in Fig. 1. This particular initiator was chosen instead of the

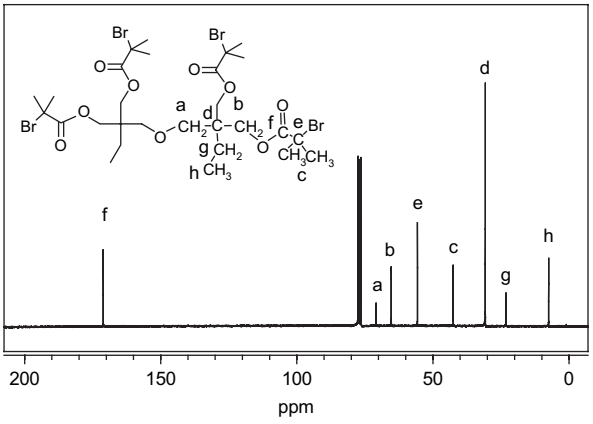

Fig. 1. ^{13}C NMR spectrum of the tetrafunctional initiator, diTMP–Br, used in the synthesis of a starlike polymer by ATRP.

often-used pentaerythritol-based one, due to its lower steric hindrance and better solubility in the monomer.

The number of arms, f, was calculated from ^{1}H NMR spectrum of the starlike poly(*tert*-butyl acrylate) using the signals of the initiator (enlarged in Fig. 2(a)) at 3.0–4.2 ppm and the signal from the endgroups of the polymer at 1.11 ppm, which gave $f = 4.05$. This polymer, (P(tBA)$_4$), was used as a macroinitiator in the copolymerisation of styrene in bulk. The aim was to attain 10 mol% polystyrene content of the block copolymer. Some fractionation of the polymer occurred during the precipitation and hence, the gravimetric determination of the conversion and thus the theoretical molar mass was not possible. After the purification the polystyrene content of the block copolymer was 8.1 mol%. The polystyrene content was calculated from ^{1}H NMR spectrum of the block copolymer shown in Fig. 2(b), using the aromatic signals of the polystyrene block at 6.2–7.2 ppm (5H) and the signal of poly(*tert*-butyl acrylate) at 2.24 ppm (1H). The molar masses of the (P(tBA)$_4$) macroinitiator, as well as the purified block copolymer are presented in Table 1, and the corresponding size exclusion chromatograms are shown in Fig. 3. Using the M_n values determined by NMR for (P(tBA)$_4$) and (ptBA-*b*-PS)$_4$, the average degree of polymerization is 54 for the ptBA block and 6 for the PS block (Table 1).

Table 1
Molecular characteristics of the star polymers

Polymer	Conversion [%]	M_n(theor)[a] [g/mol]	M_n(NMR) [g/mol]	M_n(SEC) [g/mol]	PDI
(P(tBA)$_4$)	64.0	26,200	27,700	27,000	1.19
(ptBA-*b*-PS)$_4$			30,100	30,300	1.15
(PAA-*b*-PS)$_4$			23,100[b]	23,500[b]	1.15

[a] M_n(theor) = [M]/[I] × conversion × M(monomer) + M(initiator).
[b] Calculated according to 97% hydrolysis of *tert*-butyl ester group.

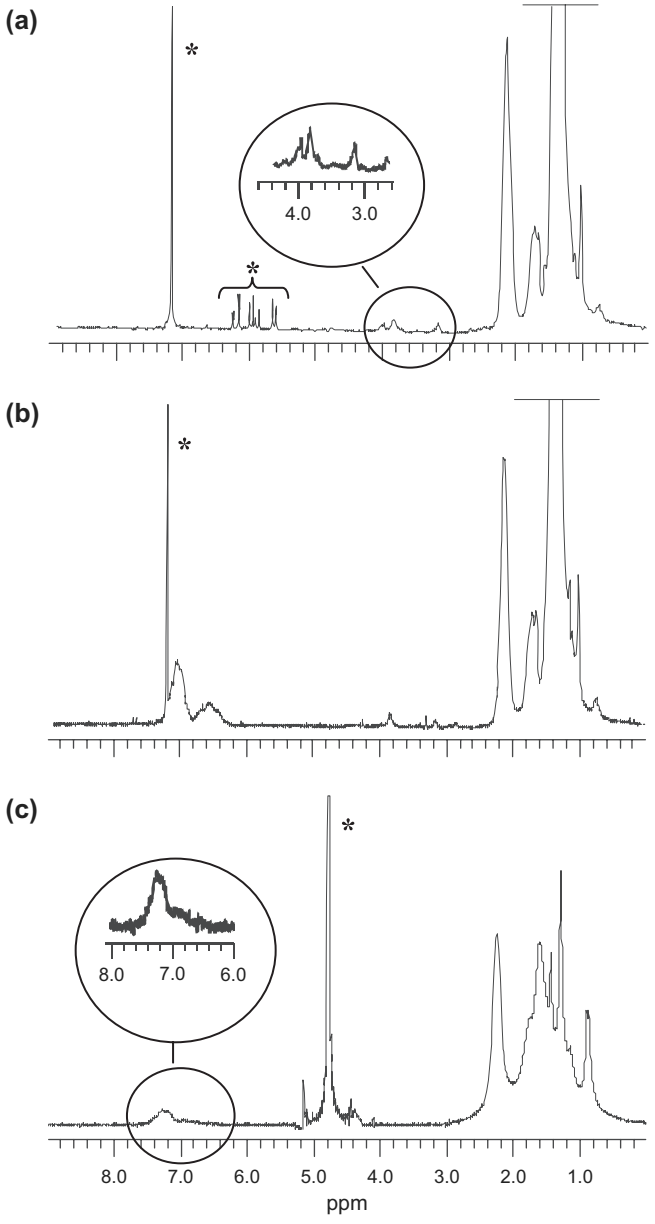

Fig. 2. ^{1}H NMR spectra of (a) (P(tBA)$_4$) in $CDCl_3$, (b) (ptBA-*b*-PS)$_4$ in $CDCl_3$, and (c) (PAA-*b*-PS)$_4$ in D_2O (polymer concentration 10 g/L). The smallest signals, the ones from the initiator in (a) and the aromatic signals in (c), have been enlarged. The spectral assignments are presented in Section 2. The signals from the solvents or from impurities (monomer) are marked with asterisks.

The amphiphilisation of the star block copolymer was conducted by the hydrolysis of *tert*-butyl ester groups with trifluoroacetic acid. The presence of –OH groups in the purified amphiphile is clearly observed as a broad band at $\nu = 3395\ cm^{-1}$ in the FT-IR spectrum presented in Fig. 4. Based on the composition of the (ptBA-*b*-PS)$_4$ precursor, the amphiphilic (PAA-*b*-PS)$_4$ polymer is denoted as (PAA$_{54}$-*b*-PS$_6$)$_4$. The ^{1}H NMR spectrum of the (PAA-*b*-PS)$_4$ star in D_2O is shown in Fig. 2(c). The extent of hydrolysis was estimated from the ^{1}H NMR spectra of the purified polymer, being 97%. Despite the fact that polystyrene blocks are insoluble in water, their aromatic signals are visible in the spectrum of 10 g/L solution in D_2O, suggesting that they retain some of their mobility. This is expected as the theoretical T_g for

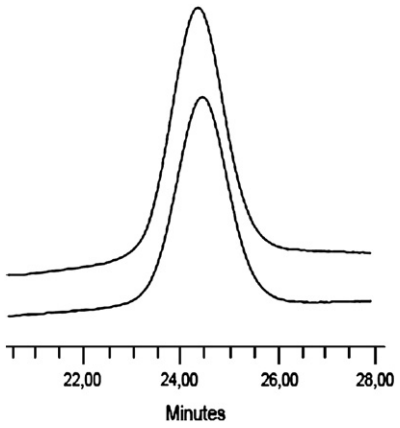

Fig. 3. Size exclusion chromatograms of (P(tBA)$_4$) M_n(SEC) = 27,000 g/mol (below) and (ptBA-*b*-PS)$_4$ after the fractionation M_n(SEC) = 30,300 g/mol (above).

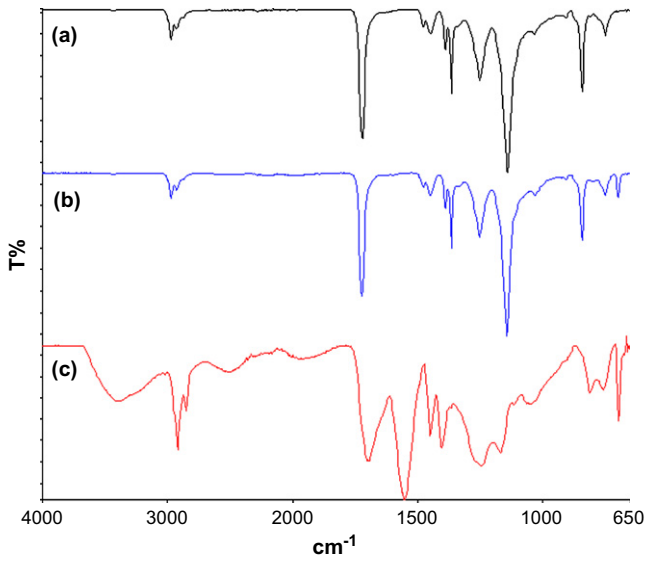

Fig. 4. FT-IR spectra of starlike (a) (P(*t*BA)$_4$), (b) (p*t*BA-*b*-PS)$_4$, and (c) (PAA-*b*-PS)$_4$. The wavenumbers of the bands as well as the assignments for the most important bands are listed in Section 2.

a polystyrene with degree of polymerization of around 6 would be around −20 °C [39].

3.2. Effect of polymer concentration on the rheological properties of (PAA_{54}-b-PS_6)$_4$

Solution of the polymer in water behaves liquid-like at polymer concentrations (C_p) below 20 g/L at 20 °C. This is seen in the rheological measurements (Fig. 5) as the loss modulus G'' is larger than the storage modulus G' throughout the measured range of oscillation frequencies. However, at C_p = 20–22 g/L the scaling of the moduli are almost parallel and differ from the typical scaling behaviour a viscous liquid, where $G' \sim \omega^2$ and $G'' \sim \omega$. At C_p above 22 g/L the frequency sweeps show that G' is larger than G'' at oscillation frequencies above 0.1 rad/s, see Fig. 5. This development of the moduli upon increasing concentration indicates a strongly correlated behaviour at C_p 20–22 g/L and suggests a self-similar behaviour in the sense of a large-scale organization. This state can be described as a precursor state for the gel formation, analogous to studies by Mallamace et al. [40] and Ozon et al. [41], where a precursor state has been observed for thermally induced gelation of block copolymers of poly(ethylene oxide)–poly(propylene oxide)–poly(ethylene oxide) in water [40] and for a multiarm star 1,4-polybutadiene in toluene [41].

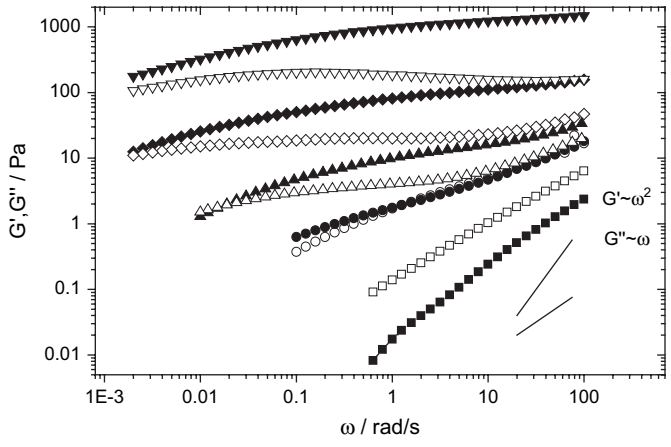

Fig. 5. Storage (G') and loss (G'') moduli of aqueous solutions at 20 °C as a function of oscillation frequency, C_p 20 g/L (G' ■, G'' □), 22 g/L (G' ●, G'' ○), 26 g/L (G' ▲, G'' △), 34 g/L(G' ◆, G'' ◇) and 51 g/L(G' ▼, G'' ▽).

When the polymer concentrations are higher than 22 g/L, samples appear visually gel-like at 20 °C, behaving as "soft gels" or, with increasing concentrations, free-standing gels in a tube-inversion test where the solutions placed in a vial remain immobile or slowly descend to the bottom of the vial when the vial is inverted. Winter and Chambon [42] have proposed a criterion of the sol–gel transition as the point where both G' and G'' scale with ω^n and thus the tan δ (i.e. G''/G') is frequency independent. This criterion has been shown to describe well both chemical [42,43] and thermoreversible [44] gelation. Examination of the present system shows that frequency independence of the tan δ values (data not shown) is not observed. As seen in Fig. 5 the frequency sweeps for solutions with C_p above 26 g/L show that the moduli would crossover at lower frequencies. Qualitatively similar results as in the present case have been obtained for thermally gelling aqueous poly(ethylene oxide)–poly(propylene oxide)–poly(ethylene oxide) (PEO–PPO–PEO) triblock copolymer solutions [45] which did not show frequency independence in the vicinity of the sol–gel transition. Also investigation of oscillatory data presented for aqueous polystyrene-*b*-poly(acrylic acid)-*b*-poly(*n*-butyl methacrylate) PS-*b*-PAA-*b*-P*n*BMA [18] solutions reveals similar frequency dependence of moduli with increasing concentration as in the present case. Thus the proposed criterion originally developed for

Table 2
Rheological parameters of the polymer solutions

Solvent	C_p [g/L]	Gel–sol temperature[a] [°C]	G' at 20 °C at 10 Hz [Pa]	Relaxation time [s]
Water	20	–	1.6	0.01/0.06/0.23[b]
Water	22	20	12	0.8[c]
Water	26	38	31	59[c]
Water	31	41	59	–
Water	34	48	143	500[d]
Water	36	54*	282	–
Water	45	–	698	–
Water	51	–	1430	8065[d]
0.1 M NaCl	34	52*	37	
0.3 M NaCl	34	51*	35	
0.5 M NaCl	34	57*	17	
0.9 M NaCl	35	–	15	

Values marked with * are calculated from linear extrapolation of the moduli at different temperatures.

[a] Defined as the crossover point of G' and G'' at 6.28 rad/s oscillation frequency.

[b] Calculated with three parameter Maxwell model.

[c] Estimated from crossover frequency.

[d] Estimated from crossover frequency with linear extrapolation of the moduli.

chemically crosslinked gels may in some cases fail in the case of physical network systems although gel-like characteristics are observed.

As shown in Fig. 5 and Table 2, the moduli build up quickly with increasing polymer concentration, and the storage modulus reaches the value of around 1000 Pa at C_p 51 g/L, indicating the formation of a strong elastic gel. The values of moduli for the $(PAA_{54}$-*b*-$PS_6)_4$ star block copolymer solutions are comparable to the ones of corresponding linear PANa–PS, sodium salt of PAA, diblock and triblock polymer solutions described in literature. A PS–PANa–PS triblock polymer with $M_w = 107{,}400$ g/mol and block lengths of PS_{23}–PAA_{1134}–PS_{23} was reported by Tsitsilianis et al. [16,17]. Their system showed remarkably low gelling concentration, 0.2 wt%, and relatively high storage modulus, G', of 1000 Pa at C_p 10 g/L. These authors point out that G' may be partly affected by unhydrolyzed *t*BA units. However, the lower gelling concentration and higher modulus at lower polymer concentration of the PS_{23}–PAA_{1134}–PS_{23} compared to $(PAA_{54}$-*b*-$PS_6)_4$ may be attributed to longer lengths of the hydrophobic blocks and higher molecular weight of the triblock polymer and different topologies of the systems, as starlike polymer is likely to have a smaller hydrodynamic size than a corresponding linear one.

Bhatia and Mourchid [14] found a gelation threshold within a narrow concentration range between 1.13 and 1.4 wt% for their diblock PS–PAA with molecular weights of the blocks PS 5300 g/mol and PAA 6170 g/mol. The PAA block of the PS–PAA was hydrolysed to 85%, the rest being remaining poly(ethyl acrylate), thus leading to increased hydrophobicity. The gel elasticity, $G' \sim 1$–10 Pa, at the gelling point was on the same level as in the current study and in the work of Tsitsilianis et al. [16]. The lower gelling concentration of the PS–PAA compared with the $(PAA_{54}$-*b*-$PS_6)_4$ may be explained by the more hydrophobic nature of the PS–PAA polymer, having higher polystyrene content and remaining ethyl acrylate groups. In addition, a linear diblock copolymer is supposed to form a gel via micellar aggregation whereas starlike block copolymers or linear triblock copolymers may form gels in addition via physical intermolecular crosslinking [31]. Therefore the gelling characteristics of linear and starlike diblock copolymers are not directly comparable with each other.

The scaling of the complex viscosity $|\eta^*|$ and the plateau modulus G_0 with concentrations at 0.1 rad/s for $|\eta^*|$ and 62.8 rad/s for G_0 were analyzed by following the approach used by Tsitsilianis and Iliopoulos [17]. The evolution of these parameters with concentration is plotted in Fig. 6 for $(PAA_{54}$-*b*-$PS_6)_4$ solutions. High scaling exponents of 7.1 and 5.9 for the $|\eta^*|$ and G_0, respectively, were found. These values are close to the values found for the PS_{23}–PAA_{1134}–PS_{23} triblock copolymer [17] (5.9 for $|\eta^*|$ and 4.7 for G_0). As pointed out by Tsitsilianis et al. [16], these scaling relationship values differ remarkably from linear PAA which has a scaling relation of the viscosity as a function of polymer concentration of 0.53, close to the theoretical prediction for polyelectrolytes in the semidilute regime. The scaling relation obtained for the

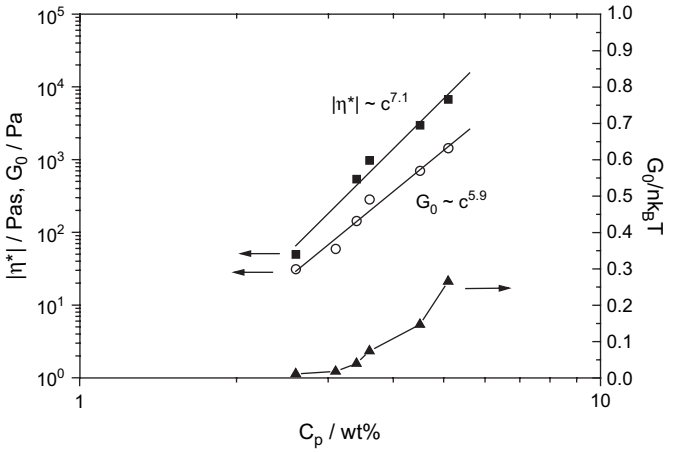

Fig. 6. Scaling of $|\eta^*|$ at 1 rad/s (■), G_0 at 62.8 rad/s (○) and the reduced modulus (▲) as a function of polymer concentration.

$(PAA_{54}$-*b*-$PS_6)_4$ with relatively low molecular weight and at such low concentration is attributed to the physical network formation due to the PS sticker groups. In addition the starlike topology of the $(PAA_{54}$-*b*-$PS_6)_4$ may contribute to the higher scaling relation in the current study compared with the PS_{23}–PAA_{1134}–PS_{23} triblock copolymer [17], as the scaling relations for starlike polymers differ significantly from corresponding linear chains [46].

According to the Green–Tobolsky theory on rubber elasticity [47], the plateau modulus G_0 is given by

$$G_0 = g\nu k_B T \tag{1}$$

where g is the correction factor usually taken as unity for systems with large junction functionality, ν is the number density of elastically active chains, k_B is the Boltzmann constant and T is the absolute temperature. For unentangled networks as in the present system the fraction of bridging, elastically active chains between the hydrophobic cores, ν/n, is also called the reduced modulus and is given by

$$\nu/n = G_0/nk_B T \tag{2}$$

where n denotes the number density of total chains in the solution, calculated by using the number of star molecules. By using this approach, shown in Fig. 6, it can be seen that the reduced modulus for the $(PAA_{54}$-*b*-$PS_6)_4$ solutions increases monotonically with increasing concentration, but remains well below unity. The values below unity in the present case resemble the data reported for nonionic hydrophobically modified PEO with hexadecyl or octadecyl hydrophobes at both chain ends by Pham et al. [30] and hydrophobically modified polyetherurethanes by Annable et al. [32] and differ significantly from the work of Tsitsilianis and Iliopoulos [17] where values of reduced modulus up to almost nine were observed. The values of reduced moduli of the hydrophobically modified PEO were rationalized by assuming that excluded volume interactions and the micellar structure may also be important and that the structure and interactions of the systems may be interpreted in terms of behaviour of flowerlike micelles. We

conclude that for the polymers in the present case the aggregation of the starlike amphiphiles reduces the fraction of the elastically active chains available for intermolecular association. Also, the close proximity of the PS-stickers in the case of these relatively small star polymers may cause intramolecular association. These effects may lead to the observed lower reduced moduli than in the case of PS_{23}–PAA_{1134}–PS_{23} triblock copolymer [17].

In order to estimate the lifetime of the hydrophobic junctions we use the oscillatory data for the determination of relaxation times. For the sample with C_p 20 g/L the moduli may be adequately fitted with three Maxwell elements according to

$$G'(\omega) = G_0 \sum_{i=1}^{3} \frac{\omega^2 \tau_i^2}{1+\omega^2\tau_i^2} \quad G''(\omega) = G_0 \sum_{i=1}^{3} \frac{\omega \tau_i}{1+\omega^2\tau_i^2} \tag{3}$$

where τ_i is the relaxation time. For this sample, three relaxation times $\tau_1 = 0.01$ s, $\tau_2 = 0.06$ s and $\tau_3 = 0.24$ s were obtained. Of these relaxation times the τ_3 can be identified as the slow mode of the system and thus representing the lifetime of the junctions in the hydrophobic clusters [5]. However, for samples at and above C_p 22 g/L the data do not fit well to the Maxwell model due to a broad distribution of relaxation times. In order to get a rough estimation of the terminal relaxation time for these samples, we use the crossover frequency of the moduli as an indicator of the terminal relaxation time and thus representing the dissociation of the hydrophobic associations [5]. From Fig. 5 it can be seen how the crossover frequency decreases with increasing C_p. The relaxation times in Table 2 show values from ~0.8 s for C_p 22 g/L increasing to 8000 s for the highest studied concentration (51 g/L) sample.

3.3. Effect of temperature on the rheological behaviour

The dependence of the moduli on temperature of the $(PAA_{54}$-*b*-$PS_6)_4$ hydrogel is seen in Fig. 7, presenting the temperature sweep performed at a single frequency of 6.28 rad/s on the 26 g/L sample. The storage modulus G' is around 17 Pa at 20 °C and starts to decrease rapidly with increasing temperature. The reduced modulus, although now determined from G' at 6.28 rad/s frequency, is seen to decrease at the same time. The same behaviour was noted throughout the studied concentrations at higher frequencies (data not shown).

In Fig. 7 the storage and loss moduli cross each other at 38 °C which is taken as the gel-to-solution temperature (gel–sol) for the 26 g/L sample. As can be seen from Table 2, the other concentrations in water show similar gel–sol behaviour, apart from the sample that behaves as a viscous liquid at 20 °C (20 g/L) or those which have such high concentrations (>45 g/L) that the moduli at 6.28 rad/s do not cross within the measured temperature range.

A clear trend of higher gel–sol temperatures with increasing C_p is seen in Table 2. Both the changes in the moduli and the temperature of the gel–sol transition may be interpreted as originating from the increased number of transient junctions between the hydrophobes with increasing C_p. Tsitsilianis and Iliopoulos [17] studied the earlier mentioned PS_{23}–PAA_{1134}–PS_{23} by stress relaxation measurements at increasing temperatures and found a decreasing plateau modulus and network relaxation time following Arrhenius behaviour. As in the present case, they found that the higher studied concentration of PS_{23}–PAA_{1134}–PS_{23} (1 wt%) in water remained as gel at 50 °C. However, the effect of concentration on the possible gel–sol behaviour at lower concentrations was not discussed.

3.4. Effect of ionic strength on the rheological behaviour

The effect of ionic strength on the rheological properties of the $(PAA_{54}$-*b*-$PS_6)_4$ polymer solutions is shown in Fig. 8. Samples with 34 g/L concentration were selected due to their gel–sol temperature within the easily accessible measuring range. Fig. 8 and Table 2 show the samples having lower values of moduli with increasing salinity of the solution. Nevertheless, the samples are gels at 20 °C up to the studied NaCl

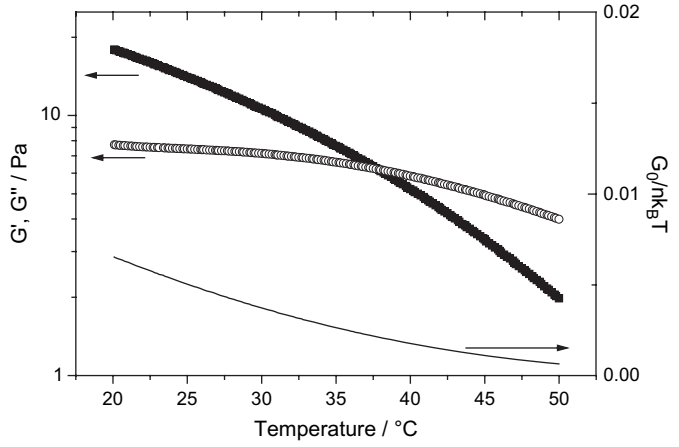

Fig. 7. Storage (■) and loss (○) modulus of the 26 g/L sample in water at 6.28 rad/s oscillation frequency. On the right axis is shown the reduced modulus calculated from the G' at 6.28 rad/s. The heating rate is 1 °C/min.

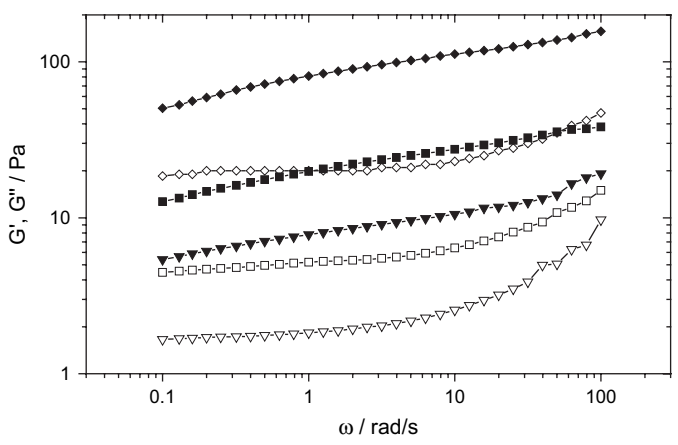

Fig. 8. Storage (G') and loss (G'') moduli of the 34 g/L solutions at 20 °C as a function of oscillation frequency. Water (G' ◆, G'' ◇), 0.1 M NaCl (G' ■, G'' □), 0.5 M NaCl (G' ▼, G'' ▽).

concentration of 0.9 M and no precipitation of the polymer was observed. Decreasing elasticity and viscosity are expected to occur in such a system, as the electrostatic screening of the PANa blocks is likely to allow more flexibility of the polyelectrolyte chains and lead to more contracted dimensions of the molecules. Indeed, similar behaviour was reported by Kimerling et al. [2] for a 1 wt% solution of diblock PS–PAA (PS 1400 g/mol, PAA 40,200 g/mol) in 0.020 M NaOH. For the PS–PAA samples a very small addition of NaCl (0.0009–0.099 M) lead to significantly decreased viscosity and moduli. In the present case, the decrease upon salt addition is much less pronounced. In spite of the fact that the degree of ionization was adjusted with NaOH in Ref. [2], the observed difference in the effect of salt is important. Once again this shows that the topology of the polymer affects its behaviour and the star topology having smaller hydrodynamic dimensions and less conformational freedom leads to less pronounced effect upon salt addition.

On the other hand, as shown in Table 2, the gel–sol temperature of the saline solutions does not change significantly with salt concentration, but rather keeps more or less the same. These two effects, decreasing moduli and the unchanged gel–sol temperature, show that upon addition of salt the electrostatic screening of the polyelectrolyte part is the governing factor behind the decreasing modulus. Secondly, the observed temperature dependence originates from the number of hydrophobic network junctions, which is not likely to change significantly upon addition of salt.

3.5. Flow behaviour of the solutions

In comparison to linear oscillatory shear measurements, the flow behaviour of the polymer solutions was studied by steady shear measurements. The flow viscosities of the polymer solutions in water at 20 °C are depicted in Fig. 9. The solutions below gelling C_p at 20 °C of 22 g/L have relatively low viscosities with slight shear thinning at high shear rates. Upon increase in the polymer concentration, the viscosity is significantly enhanced as already shown by oscillatory measurements. The shape of the flow curve of the 22 g/L sample is typical for hydrophobically modified polymers, showing a characteristic slightly increasing viscosity with shear rate increasing from 0.1 to 0.5 s^{-1} and strong shear thinning at higher shear rates. For the higher concentrations studied (26 and 34 g/L) the upward change in viscosity is not as obvious but a slight change in the slope may be observed before the strong shear thinning region at shear rates above 10 s^{-1}. Although the phenomenon behind the increasing viscosity at low shear rates is poorly understood, it may be speculated that the upturn indicates increase of the elastically active chains upon shearing. Upon shearing the transient network is disrupted into associative clusters and further to smaller fragments which leads to the observed shear thinning behaviour. The discontinuity observed in the flow curves (e.g. 70 Pa for $C_p = 26$ g/L) in the inset of Fig. 9 at a critical shear stress has been reported for other associating polymers [9,22] and can be ascribed to a total destruction of the associating network structure. After the initial destruction of the network structure, a second discontinuity (e.g. around 150 Pa for $C_p = 26$ g/L) can be seen in the flow curve with less pronounced shear thinning.

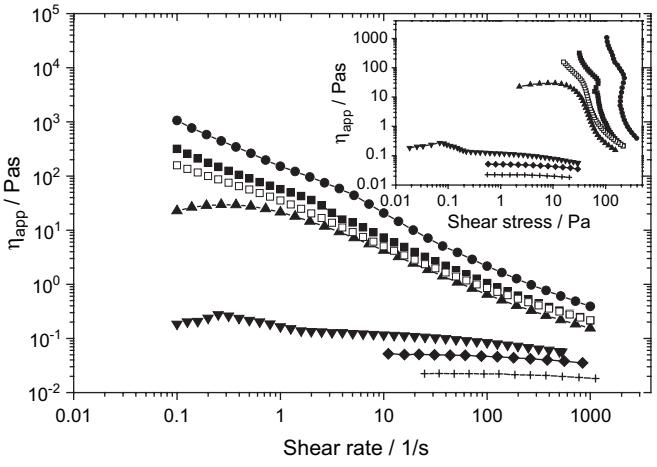

Fig. 9. Steady shear viscosity of aqueous solutions at 20 °C, C_p 11 g/L (+), 15 g/L (◆) 20 g/L (▼), 22 g/L (▲), 26 g/L (■) and 34 g/L (●).

This model of shear induced destruction of the network structure is further supported by the thixotropic response of the 26 g/L sample, which was tested by ramping down the shear rate after the initial shearing. The flow curve of the 26 g/L sample shows hysteresis when approaching lower shear rates, leading to lower apparent viscosity at lower shear rates. The onset of the hysteresis is around the second discontinuity observed at increasing shear rate indicating that the shear fractured network does not recover instantaneously during the decreasing shear. However, after equilibration for 10 min, increasing and decreasing shear rate data could be fully reproduced, showing that the structure had recovered. Due to the relatively low hysteresis it is, however, likely that the network already starts to build up during the measurement at decreasing shear rate below the discontinuity. For polymer concentrations higher than 34 g/L, the steady shear measurements at 20 °C were complicated due to the high elasticity of the gels, which lead to the slipping of the cone. For polymer concentrations above the C_p 26 g/L it is likely that the samples exhibit apparent yield stress, as observed for PS–PANa–PS triblock copolymer [16], however, the existence of yield stress was not studied further for the present system.

3.6. SAXS studies of the gels

In order to probe the structure of the polymer solutions small-angle X-ray scattering (SAXS) measurements were conducted. Aqueous solutions of $(PAA_{54}\text{-}b\text{-}PS_6)_4$ with C_p of 26, 35 and 50 g/L were inspected at 25 °C as shown in Fig. 10. For all studied samples correlation peaks in the scattering curves at $q = 0.035$ Å^{-1} and $q = 0.1$ Å^{-1} can be observed. The peak at $q = 0.035$ Å^{-1} intensifies with increasing concentration, while the peak at $q = 0.1$ Å^{-1} does not change. A peak

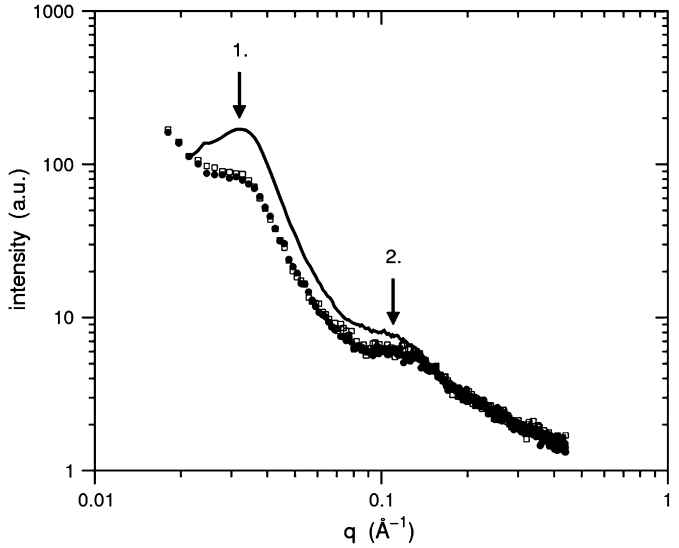

Fig. 10. SAXS curves of the star polymer in water at three polymer concentrations: 26 g/L (●), 35 g/L (○), and 50 g/L (solid line). Numbers refer to the scattering maxima at $q = 0.035$ Å^{-1} and $q = 0.1$ Å^{-1}.

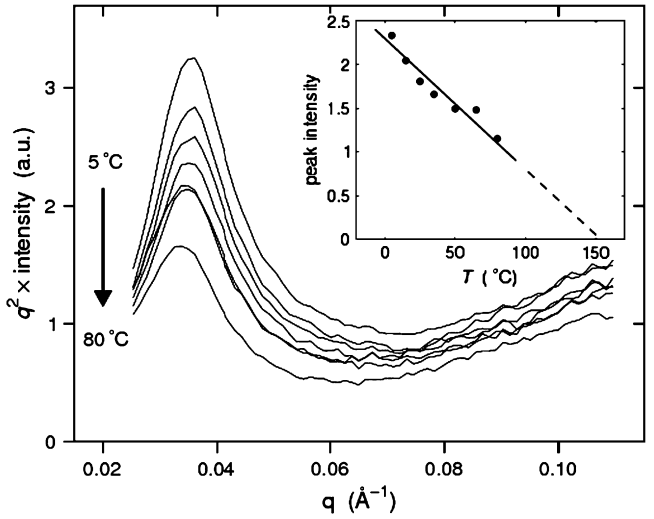

Fig. 11. SAXS curves obtained at different temperatures for the star polymer, $C_p = 50$ g/L. The inset shows the temperature dependence of the intensity of the scattering maxima at $q = 0.035$ Å^{-1}.

observed at small angles is a general feature in solutions of polyacids and with homopolymer PAA gels is typically observed at $q \sim 0.04$ Å^{-1} irrespective of the molar mass [48] but shifts towards $q = 0$ for decreased concentration or added salt. This peak is said to originate from microphase separation into polymer rich and poor domains with periodicity $2\pi/q$. A similar peak is observed furthermore in diblock PAA–PS, where it is attributed to intermicellar distances via hard sphere interactions [10]. In the present case, the peak position remains almost unchanged for the studied, albeit narrow, concentration regime and would correspond to particles of ca. 18 nm diameter, if interpreted with the hard sphere model. The contour length of a single fully stretched arm of $(PAA_{54}$-b-$PS_6)_4$ is roughly 15 nm and the lengths of PAA and PS blocks are ~13.7 and ~1.5 nm, respectively. Thus the maximum dimension of a star molecule is about 30 nm. The observed correlation distance (18 nm) is realized by assuming slightly contracted polyelectrolyte arms bridging the PS hydrophobe aggregates. Since the overall fraction of PS is small, between 0.2 and 0.5 vol% the hypothetical hydrophobe aggregates are not expected to contribute visibly to the observed intensities. Based on volume fraction, the calculated size (diameter) for the aggregates is 4–6 nm but this is most likely an overestimate in view of the block length (1.5 nm).

SAXS measurements were also conducted at different temperatures for the 50 g/L sample as shown in Fig. 11. From the data it can be seen that both the $q = 0.035$ Å^{-1} and $q = 0.1$ Å^{-1} peaks are present throughout the measuring temperatures but the intensity of the $q = 0.035$ Å^{-1} peak diminishes with increasing temperature and shifts slightly to lower q values while the $q = 0.1$ Å^{-1} peak does not change significantly. This result may be taken as an indication of the increased thermal motion in the system that reduces the number of the transient crosslinks with increasing temperature. At the same time, the observed decrease by a factor of two within 80 degrees is more or less the same as for the homopolymer PAA [46]. This result is in agreement with the rheological data and shows that the samples undergo a smooth gel–sol transition in this temperature range.

4. Conclusions

A water-soluble amphiphilic star polymer, $(PAA_{54}$-b-$PS_6)_4$, based on poly(acrylic acid) and polystyrene was synthesised and its rheological properties were studied in aqueous solutions. In water the polymer formed hydrogels with increasing polymer concentration (C_p). The gelling concentration in water was found to be 22 g/L and elastic gels (storage modulus > 1100 Pa) were observed at the highest studied C_p of 51 g/L. The observed physical network formation at such low concentrations was rationalized by the transient interpolymer hydrophobic association of the PS blocks and the starlike topology of the polymers. Upon addition of NaCl (0.1–0.9 M) the viscoelastic moduli decreased compared with aqueous solutions but samples behaved as gels at 20 °C at the studied C_p of 34 g/L, showing that the polyelectrolyte screening upon salt addition shrunk the PAA chains but did not affect the hydrophobic association. Gel-to-solution transition (gel–sol) with increased temperature (20–57 °C) was observed for the gels, the gel–sol temperature increasing with increasing C_p. For the studied saline solutions the gel–sol transition temperature did not change compared with the aqueous solutions of the same C_p, again indicating that the hydrophobic association was not affected by salt addition. Small-angle X-ray experiments showed two distinct scattering correlation peaks for samples above the gelling C_p. Upon heating the scattering intensity decreased strongly and the scattering correlation peak maximum shifted slightly to lower values of scattering vector. The SAXS results are thus in agreement with the rheological studies, showing the formation of a transient network which is partly broken upon heating.

Acknowledgment

S. Strandman wishes to thank the Finnish National Graduate School in Nanoscience (NGS-NANO) for funding.

References

[1] Glass JE, editor. Hydrophilic polymers: performance with environmental acceptability, advances in chemistry series 248. Washington, DC: American Chemical Society; 1996.
[2] Kimerling AS, Rochefort WE, Bhatia SR. Ind Eng Chem Res 2006;45: 6885–9.
[3] Cohen Stuart MA, Hofs B, Voets IK, de Keizer A. Curr Opin Colloid Interface Sci 2005;10:30–6.
[4] Xue W, Hamley IW, Castelletto V, Olmsted PD. Eur Polym J 2004;40: 47–56.
[5] Castelletto V, Hamley IW, Xue W, Sommer C, Pedersen JS, Olmsted PD. Macromolecules 2004;37:1492–501.
[6] Ricardo NMPS, Honorato SB, Yang Z, Castelletto V, Hamley IW, Yuan X-F, et al. Langmuir 2004;20:4272–8.
[7] Couillet I, Hughes T, Maitland G, Candau F. Macromolecules 2005;38: 5271–82.
[8] English RJ, Gulati HS, Jenkins RD, Khan SA. J Rheol 1997;41: 427–44.
[9] Kujawa P, Audibert-Hayet A, Selb J, Candau F. J Polym Sci Part B Polym Phys 2004;42:1640–55.
[10] Korobko AV, Jesse W, Lapp A, Egelhaaf SU, van der Maarel JRC. J Chem Phys 2005;122:024902.
[11] McCormick CL, Middleton JC, Cummins DF. Macromolecules 1992;25: 1201–6.
[12] Borrega R, Tribet C, Audebert R. Macromolecules 1999;32:7798–806.
[13] Yang Y, Schulz D, Steiner CA. Langmuir 1999;15:4335–43.
[14] Bhatia SR, Mourchid A. Langmuir 2002;18:6469–72.
[15] Tsitsilianis C, Katsampas I, Sfika V. Macromolecules 2000;33: 9054–9.
[16] Tsitsilianis C, Iliopoulos I, Ducouret G. Macromolecules 2000;33: 2936–43.
[17] Tsitsilianis C, Iliopoulos I. Macromolecules 2002;35:3662–7.
[18] Katsampas I, Tsitsilianis C. Macromolecules 2005;38:1307–14.
[19] Castelletto V, Hamley IW, Ma Y, Bories-Azeau X, Armes SP, Lewis AL. Langmuir 2004;20:4306–9.
[20] Voulgaris D, Tsitsilianis C. Macromol Chem Phys 2001;202:3284–92.
[21] Park SY, Han DK, Kim SC. Macromolecules 2001;34:8821–4.
[22] Tam KC, Farmer ML, Jenkins RD, Bassett DR. J Polym Sci Part B Polym Phys 1998;36:2275–90.
[23] Li Y, Tang Y, Narain R, Lewis AL, Armes SP. Langmuir 2005;21: 9946–54.
[24] Li Y, Narain R, Ma Y, Lewis AL, Armes SP. Chem Commun 2004; 2746–7.
[25] Li C, Buurma NJ, Haq I, Turner C, Armes SP, Castelletto V, et al. Langmuir 2005;21:11026–33.
[26] Bromberg L. Langmuir 1998;14:5806–12.
[27] Noda T, Hashidzume A, Morishima Y. Langmuir 2000;16:5324–32.
[28] Kujawa P, Audibert-Hayet A, Selb J, Candau F. Macromolecules 2006; 39:384–92.
[29] Bossard F, Aubry T, Gotzamanis G, Tsitsilianis C. Soft Matter 2006;2: 510–6.
[30] Pham QT, Russel WB, Thibeault JC, Lau W. Macromolecules 1999;32: 5139–46.
[31] Lin H-H, Cheng Y-L. Macromolecules 2001;34:3710–5.
[32] Annable T, Buscall R, Ettelaie R. Colloids Surf A Physicochem Eng Asp 1996;112:97–116.
[33] Ternat C, Kreutzer G, Plummer CJG, Nguyen TQ, Herrmann A, Ouali L, et al. Macromol Chem Phys 2007;208:131–45.
[34] Kanaoka S, Nakata S, Yamaoka H. Macromolecules 2002;35:4564–6.
[35] Terashima T, Ouchi M, Ando T, Kamigaito M, Sawamoto M. J Polym Sci Part A Polym Chem 2006;44:4966–80.
[36] Dichtel WR, Baek K-Y, Frechet JMJ, Rietveld IB, Vinogradov SA. J Polym Sci Part A Polym Chem 2006;44:4939–51.
[37] Jankova K, Bednarek M, Hvilsted S. J Polym Sci Part A Polym Chem 2005;43:3748–59.
[38] Ma Q, Wooley K. J Polym Sci Part A Polym Chem 2000;38:4805–20.
[39] O'Driscoll K, Amin Sanayei R. Macromolecules 1991;24:4479–80.
[40] Mallamace F, Chen S-H, Liu Y, Lobry L, Micali N. Physica A 1999;266: 123–35.
[41] Ozon F, Petekidis G, Vlassopoulos D. Ind Eng Chem Res 2006;45: 6946–52.
[42] Chambon F, Winter HH. Polym Bull 1985;13:499.
[43] Winter HH, Mours M. Adv Polym Sci 1997;134:165–234.
[44] te Nijenhuis K, Winter HH. Macromolecules 1989;22:411–4.
[45] Nyström B, Walderhaug H. J Phys Chem 1996;100:5433–9.
[46] Vlassopoulos D. J Polym Sci Part B Polym Phys 2004;42:2931–41.
[47] Green MS, Tobolsky AV. J Chem Phys 1946;14:80–92.
[48] Moussaid A, Schlosseler F, Munch JP, Candau SJ. J Phys II 1993;3: 573–94.